

QUANTILED CONDITIONAL VARIANCE, SKEWNESS, AND KURTOSIS BY CORNISH-FISHER EXPANSION

NINGNING ZHANG AND KE ZHU*

University of Hong Kong

The conditional variance, skewness, and kurtosis play a central role in time series analysis. These three conditional moments (CMs) are often studied by some parametric models but with two big issues: the risk of model mis-specification and the instability of model estimation. To avoid the above two issues, this paper proposes a novel method to estimate these three CMs by the so-called quantiled CMs (QCMs). The QCM method first adopts the idea of Cornish-Fisher expansion to construct a linear regression model, based on n different estimated conditional quantiles. Next, it computes the QCMs simply and simultaneously by using the ordinary least squares estimator of this regression model, without any prior estimation of the conditional mean. Under certain conditions that allow estimated conditional quantiles to be biased, the QCMs are shown to be consistent with the convergence rate $n^{-1/2}$. Simulation studies indicate that the QCMs perform well under different scenarios of estimated conditional quantiles. In the application, the study of QCMs for eight major stock indexes demonstrates the effectiveness of financial rescue plans during the COVID-19 pandemic outbreak, and unveils a new “non-zero kink” phenomenon in the “news impact curve” function for the conditional kurtosis.

*Address correspondence to Ke Zhu: Department of Statistics and Actuarial Science, University of Hong Kong, Hong Kong. E-mail: mazhuke@hku.hk

Keywords: Conditional moments; Cornish-Fisher expansion; News impact curve; Quantile time series estimation; Quantiled conditional moments.

1. Introduction. Learning the conditional variance, skewness, and kurtosis of a univariate time series is the core issue in many financial and economic applications. The classical tools to study the conditional variance are the generalized autoregressive conditional heteroscedasticity (GARCH) model and its variants. See [Engle \(1982\)](#), [Bollerslev \(1986\)](#), [Francq and Zakoïan \(2019\)](#), and references therein. However, except for some theoretical works on parameter estimation in [Escanciano \(2009\)](#) and [Francq and Thieu \(2019\)](#), the GARCH-type models commonly assume independent and identically distributed (i.i.d.) innovations, resulting in the constant conditional skewness and kurtosis. As argued by [Samuelson \(1970\)](#) and [Rubinstein \(1973\)](#), the higher moments like skewness and kurtosis are nonnegligible, since they are not only exemplary evidence of the non-normal returns but also relevant to the investor’s optimal decision. Along this way, a large body of literature has demonstrated the importance of conditional skewness and kurtosis in portfolio selection ([Chunhachinda et al., 1997](#)), asset pricing ([Harvey and Siddique, 2000](#)), risk management ([Bali et al., 2008](#)), return predictability ([Jondeau et al., 2019](#)), and many others. These empirical successes indicate the necessity to learn the dynamic structures of the conditional skewness and kurtosis simultaneously with the conditional variance.

Although there is a large number of studies on the conditional variance, only a few of them have taken account of the conditional skewness and kurtosis. The pioneer works towards this goal are [Hansen \(1994\)](#) and [Harvey and Siddique \(1999\)](#), followed by [Jondeau and Rockinger \(2003\)](#), [Brooks et al. \(2005\)](#), [León et al. \(2005\)](#), [Grigoletto and Lisi \(2009\)](#), and [León and Níguez \(2020\)](#). All of these works assume a peculiar conditional distribution on the innovations of GARCH-type model, where the conditional skewness or kurtosis either directly has an analogous GARCH-type dynamic structure rooting in re-scaled shocks or indirectly depends on dynamic structure of distribution parameters. See also [Francq and Sucarrat \(2022\)](#) and [Sucarrat and Grønneberg \(2022\)](#) for a different investigation of conditional skewness and kurtosis via the GARCH-type model with a time-varying probability of zero returns. However,

the aforementioned parametric methods have two major shortcomings: First, they inevitably have the risk of using wrongly specified parametric models or innovation distributions; Second, they usually have unstable model estimation results in the presence of dynamic structure of skewness and kurtosis.

This paper proposes a new novel method to simultaneously learn the conditional variance, skewness, and kurtosis by the so-called quantiled conditional variance, skewness, and kurtosis, respectively. Our three quantiled conditional moments (QCMs) are formed based on the spirit of the Cornish-Fisher expansion ([Cornish and Fisher, 1938](#)), which exhibits a fundamental relationship between the conditional quantiles and CMs. By replacing the unknown conditional quantiles with their estimators at n quantile levels, the QCMs (with respect to variance, skewness, and kurtosis) are simply computed at each fixed timepoint by using the ordinary least squares (OLS) estimator of a linear regression model, which stems naturally from the Cornish-Fisher expansion. Surprisingly, our way to compute the QCMs does not require any estimator of the conditional mean. Under certain conditions that allow estimated conditional quantiles (ECQs) to be biased, we show that the QCMs are consistent estimators of the corresponding CMs with the convergence rate $n^{-1/2}$. Simulation studies indicate that the QCMs have a satisfactory performance using either true or contaminated or mis-specified conditional quantiles.

In the application, we study the QCMs of return series for eight major stock indexes in the U.S., Europe, and Asia. During the COVID-19 pandemic outbreak in March 2020, we find that the values of quantiled conditional variance and kurtosis increased rapidly, and the values of quantiled conditional skewness decreased sharply before March 17 or 26 in all of examined stock markets, shedding light on the worldwide perilous financial crisis at that time. After March 17 or 26, we find that the values of quantiled conditional variance, skewness, and kurtosis exhibited totally opposite trends, so demonstrating the effectiveness of financial rescue plans issued by governments. Moreover, since the existing parametric forms of “news

impact curve” (NIC) functions for the CMs are chosen in an ad-hoc way (Engle and Ng, 1993; Harvey and Siddique, 1999; León et al., 2005), we suggest a data-driven method to explore the parametric forms of the NIC functions by using the QCMs. Our suggested NIC functions for the conditional skewness and kurtosis lead to much better fittings than the existing ones. Particularly, we unveil a new “non-zero kink” phenomenon in the conditional kurtosis from our NIC function. This phenomenon is evident in most of large cap stock markets, and it implies that some small negative but non-zero past re-scaled shocks have the weakest influence on the tail risk of having extreme returns.

It is worth noting that our QCM method essentially transforms the problem of CM estimation to that of conditional quantile estimation. This brings us two major advantages over the aforementioned parametric methods, although we need do the conditional quantile estimation n different times to implement the QCM method.

First, the QCM method can largely reduce the risk of model mis-specification, since the QCMs are simultaneously computed without any prior estimation of the conditional mean, and their consistency holds even when the specifications of conditional quantiles are mis-specified. This advantage is attractive and unexpected, since we usually have to estimate conditional mean, variance, skewness (or kurtosis) successively via some correctly specified parametric models. The reason of this advantage is that the QCM method is regression-based. Specifically, the conditional mean formally becomes one part of the intercept parameter, so it has no impact on the QCMs that are computed only from the OLS estimator of all non-intercept parameters; meanwhile, the impact of biased ECQs from the use of wrongly specified conditional quantile models can be aggregately offset by another part of the intercept parameter, ensuring the consistency of QCMs to a large extent. In a sense, without specifying any parametric forms of CMs, this important feature allows us to view the QCMs as the “observed” CMs, and consequently, many intriguing but hardly implemented empirical studies could become tractable based on the QCMs (see, e.g., our empirical studies on NICs for the CMs).

Second, the QCM method can numerically deliver more stable estimators of the CMs than the parametric methods. As shown in [Jondeau and Rockinger \(2003\)](#), there exists a moment issue that places a necessary nonlinear constraint on the conditional skewness and kurtosis, leading to a complex restriction on the admission region of model parameters. This restriction not only raises the computational burden of parameter estimation but also makes the estimation result unstable, so it has been rarely considered in the existing parametric methods. In contrast, the QCM method directly computes the QCMs at each fixed timepoint, and this interesting feature ensures that the nonlinear constraint on the conditional skewness and kurtosis can be simply examined using the computed QCMs at each timepoint. Particularly, if this nonlinear constraint is violated at some timepoints, it is straightforward to replace the OLS estimator with a constrained least squares estimator to propose the QCMs which then satisfy the constraint automatically.

The remaining paper is organized as follows. Section 2 proposes the QCMs based on the linear regression, discusses the issues of conditional mean and moment constraints, and compares the proposed QCM method with the naive QCM method. Section 3 establishes the asymptotics of the QCMs. Section 4 provides the practical implementations of the QCMs. Simulation studies are given in Section 5. An application to study the QCMs for eight major index return series and their related NICs is offered in Section 6. Concluding remarks are presented in Section 7. Proofs and some additional simulation results are deferred into the supplementary materials.

2. Quantiled Conditional Moments.

2.1. *Definition.* Let $\{y_1, \dots, y_T\}$ be a time series of interest with length T , and $\mathcal{F}_t \equiv \sigma(y_s; s \leq t)$ be its available information set up to time t . Given \mathcal{F}_{t-1} , the conditional mean, variance, skewness, and kurtosis of y_t at timepoint t are defined as $\mu_t = E(y_t | \mathcal{F}_{t-1})$ and

$$(2.1) \quad h_t = E[(y_t - \mu_t)^2 | \mathcal{F}_{t-1}], \quad s_t = E\left(\left(\frac{y_t - \mu_t}{\sqrt{h_t}}\right)^3 | \mathcal{F}_{t-1}\right), \quad k_t = E\left(\left(\frac{y_t - \mu_t}{\sqrt{h_t}}\right)^4 | \mathcal{F}_{t-1}\right),$$

respectively. Below, we show how to estimate these three conditional moments in (2.1) by using the Cornish-Fisher expansion (Cornish and Fisher, 1938) at a fixed timepoint t .

Let $Q_t(\alpha)$ be the conditional quantile of y_t at the quantile level $\alpha \in (0, 1)$. According to the Cornish-Fisher expansion, we have

$$(2.2) \quad Q_t(\alpha) = \mu_t + \sqrt{h_t} \left[x + (x^2 - 1) \frac{s_t}{6} + (x^3 - 3x) \frac{k_t - 3}{24} + r_t(\alpha) \right],$$

where $x = \Phi^{-1}(\alpha)$ with $\Phi(\cdot)$ being the distribution function of $N(0, 1)$, and $r_t(\alpha)$ contains all remaining terms on the higher-order conditional moments. Taking n quantile levels α_i , $i = 1, \dots, n$, equation (2.2) entails the following regression model with deterministic explanatory variables \mathbf{X}_i but random coefficients β_t :

$$(2.3) \quad Y_{t,i}^* = \mu_t + \mathbf{X}_i' \beta_t + \varepsilon_{t,i}^*, \quad i = 1, \dots, n,$$

where $Y_{t,i}^* = Q_t(\alpha_i)$, $\mathbf{X}_i = (x_i, x_i^2 - 1, x_i^3 - 3x_i)'$ with $x_i = \Phi^{-1}(\alpha_i)$,

$$(2.4) \quad \beta_t \equiv (\beta_{1t}, \beta_{2t}, \beta_{3t})' = \left(\sqrt{h_t}, \frac{\sqrt{h_t} s_t}{6}, \frac{\sqrt{h_t} (k_t - 3)}{24} \right)',$$

and $\varepsilon_{t,i}^* = \sqrt{h_t} r_t(\alpha_i)$. We call $\varepsilon_{t,i}^*$ the expansion error, since it comes from the Cornish-Fisher expansion but can not be explained by \mathbf{X}_i adequately.

Next, we aim to obtain the estimators of h_t , s_t , and k_t through the estimator of β_t in (2.4). To achieve this goal, we replace the unobserved $Y_{t,i}^*$ with its estimator $Y_{t,i}$, and then rewrite model (2.3) as follows:

$$(2.5) \quad Y_{t,i} = \mu_t + \mathbf{X}_i' \beta_t + \varepsilon_{t,i}^\bullet, \quad i = 1, \dots, n,$$

where $Y_{t,i} = \hat{Q}_t(\alpha_i)$ with $\hat{Q}_t(\alpha_i)$ being an estimator of $Q_t(\alpha_i)$, and $\varepsilon_{t,i}^\bullet = \varepsilon_{t,i}^* + \varepsilon_{t,i}^\circ$ with $\varepsilon_{t,i}^\circ = \hat{Q}_t(\alpha_i) - Q_t(\alpha_i)$. Clearly, $\varepsilon_{t,i}^\circ$ quantifies the error caused by using $\hat{Q}_t(\alpha_i)$ to approximate $Q_t(\alpha_i)$, so it can be termed as the approximation error. Consequently, $\varepsilon_{t,i}^\bullet$ considering the total number of $\varepsilon_{t,i}^*$ and $\varepsilon_{t,i}^\circ$ can be viewed as the gross error. We should mention that any two quantile levels

α_i and α_j in (2.5) are allowed to be the same, as long as $Y_{t,i}$ and $Y_{t,j}$ are different due to the use of two different conditional quantile estimation methods. In other words, model (2.5) allows us to simply pool different information of conditional quantiles from different channels of estimation methods at any fixed quantile level.

Although $\varepsilon_{t,i}^\bullet$ is expected to have values oscillating around zero, it may not always have mean zero. Therefore, for the purpose of identification, we add a deterministic term γ_t into model (2.5) to form the following regression model:

$$(2.6) \quad Y_{t,i} = (\mu_t + \gamma_t) + \mathbf{X}_i' \boldsymbol{\beta}_t + \varepsilon_{t,i} \equiv \mathbf{Z}_i' \boldsymbol{\theta}_t + \varepsilon_{t,i}, \quad i = 1, \dots, n,$$

where $\varepsilon_{t,i} = \varepsilon_{t,i}^\bullet - \gamma_t$, $\mathbf{Z}_i = (1, \mathbf{X}_i')'$, and $\boldsymbol{\theta}_t = (\beta_{0t}, \boldsymbol{\beta}_t')'$ with the intercept parameter $\beta_{0t} = \mu_t + \gamma_t$.

Let \mathbf{Y}_t be an $n \times 1$ vector with entries $Y_{t,i}$, \mathbf{Z} be an $n \times 4$ matrix with rows \mathbf{Z}_i' , and $\boldsymbol{\varepsilon}_t$ be an $n \times 1$ vector with entries $\varepsilon_{t,i}$. Then, the ordinary least squares (OLS) estimator of $\boldsymbol{\theta}_t$ in (2.6) is

$$(2.7) \quad \hat{\boldsymbol{\theta}}_t \equiv (\hat{\beta}_{0t}, \hat{\boldsymbol{\beta}}_t')' = (\mathbf{Z}'\mathbf{Z})^{-1} \mathbf{Z}'\mathbf{Y}_t.$$

According to (2.4), we rationally use $\hat{\boldsymbol{\beta}}_t \equiv (\hat{\beta}_{1t}, \hat{\beta}_{2t}, \hat{\beta}_{3t})'$ in (2.7) to propose the estimators \hat{h}_t , \hat{s}_t , and \hat{k}_t for h_t , s_t , and k_t , respectively, where

$$(2.8) \quad \hat{h}_t = \hat{\beta}_{1t}^2, \quad \hat{s}_t = \frac{6\hat{\beta}_{2t}}{\hat{\beta}_{1t}}, \quad \text{and} \quad \hat{k}_t = \frac{24\hat{\beta}_{3t}}{\hat{\beta}_{1t}} + 3.$$

We call \hat{h}_t , \hat{s}_t , and \hat{k}_t the quantiled conditional variance, skewness, and kurtosis of y_t , since they are estimators of h_t , s_t , and k_t , by using the estimated conditional quantiles (ECQs) of y_t . Clearly, provided n different ECQs (that is, n different $Y_{t,i}$ in (2.6)), our three quantiled conditional moments (QCMs) in (2.8) are easy-to-implement, since their computation only relies on the OLS estimator $\hat{\boldsymbol{\theta}}_t$.

2.2. The conditional mean issue. Using $\hat{\beta}_{0t}$ in (2.7), we can estimate β_{0t} but not μ_t due to the presence of γ_t . Hence, we are unable to form the quantiled conditional mean of y_t to

estimate μ_t . Interestingly, our way to compute \hat{h}_t , \hat{s}_t , and \hat{k}_t does not require an estimator of μ_t . This is far beyond our expectations, since normally we have to first estimate (or model) μ_t and then h_t , s_t , and k_t .

Although the estimation of μ_t is not required to compute \hat{h}_t , \hat{s}_t , and \hat{k}_t , knowing the dynamic structure of μ_t is still important in practice. Note that μ_t is often assumed to be an unknown constant in accordance with the efficient market hypothesis, and this constant assumption can be examined by the consistent spectral tests for the martingale difference hypothesis (MDH) in [Escanciano and Velasco \(2006\)](#). If the constant assumption is rejected by these tests, the dynamic structure of μ_t manifests and is usually specified by a linear model (e.g., the autoregressive moving-average model) or a nonlinear model (e.g., the threshold autoregressive model); see [Fan and Yao \(2003\)](#) and [Tsay \(2005\)](#) for surveys. In this case, the model correctly specifies the dynamic structure of μ_t if and only if its model error is an MD sequence, a statement which can be consistently checked by two spectral tests for the MDH on unobserved model errors in [Escanciano \(2006\)](#). Hence, it is usually tractable for practitioners to come up with a valid parametric model for μ_t in most of applications.

2.3. The moment constraints issue. Note that μ_t , h_t , s_t , and k_t can be expressed in terms of the first four non-central moments m_{1t} , m_{2t} , m_{3t} , and m_{4t} of Y_t , where $m_{jt} = E(Y_t^j | \mathcal{F}_{t-1})$. Therefore, the existence of μ_t , h_t , s_t , and k_t is equivalent to that of m_{1t} , m_{2t} , m_{3t} , and m_{4t} , and the latter requires the existence of a non-decreasing function $F_t(\cdot)$ such that $m_{jt} = \int_{-\infty}^{\infty} x^j dF_t(x)$. To ensure this existence, Theorem 12.a in [Widder \(1946\)](#) indicates that the following condition must hold for m_{1t} , m_{2t} , m_{3t} , and m_{4t} :

$$(2.9) \quad \det \begin{pmatrix} m_{0t} & m_{1t} \\ m_{1t} & m_{2t} \end{pmatrix} \geq 0 \quad \text{and} \quad \det \begin{pmatrix} m_{0t} & m_{1t} & m_{2t} \\ m_{1t} & m_{2t} & m_{3t} \\ m_{2t} & m_{3t} & m_{4t} \end{pmatrix} \geq 0.$$

By some direct calculations, it is not hard to see that condition (2.9) is equivalent to

$$(2.10) \quad h_t \geq 0 \quad \text{and} \quad k_t - s_t^2 - 1 \geq 0.$$

Condition (2.10) above places two necessary moment constraints on h_t , s_t , and k_t . When h_t , s_t , and k_t are specified by some parametric models with unknown parameters, the first moment constraint usually can be easily handled, but the second moment constraint restricts the admission region of unknown parameters in a very complex way, so that the model estimation becomes quite inconvenient and unstable. This is the reason why the second moment constraint has been rarely taken into account in the literature except [Jondeau and Rockinger \(2003\)](#).

Impressively, the moment constraints issue above is not an obstacle for our QCMs, since the QCMs estimate the CMs directly at each fixed timepoint t . In view of the relationship between the QCMs and $\hat{\beta}_t$ in (2.8), we know that the QCMs satisfy two constraints in (2.10) if and only if $\hat{\beta}_{1t}^2 \geq 0$ and $\hat{\beta}_{1t}^2 - 18\hat{\beta}_{2t}^2 + 12\hat{\beta}_{1t}\hat{\beta}_{3t} \geq 0$. Since the constraint $\hat{\beta}_{1t}^2 \geq 0$ holds automatically, we indeed only need to check whether

$$(2.11) \quad \hat{\beta}_{1t}^2 - 18\hat{\beta}_{2t}^2 + 12\hat{\beta}_{1t}\hat{\beta}_{3t} \geq 0.$$

In practice, the constraint in (2.11) can be directly examined after the QCMs are computed. Our applications in Section 6 below show that this constraint holds at all examined timepoints. In other applications, if the constraint in (2.11) does not hold at some timepoints t , we can easily re-estimate θ_t in (2.6) by the constrained least squares estimation method with the constraint $\beta_{1t}^2 - 18\beta_{2t}^2 + 12\beta_{1t}\beta_{3t} \geq 0$, so that the resulting QCMs satisfy the constraint in (2.11) automatically at these timepoints.

2.4. The naive QCMs. Based on the Cornish-Fisher expansion, our method to propose the QCMs above is based on the regression model (2.6), which uses the ECQs $\hat{Q}_t(\alpha_i)$ as its response variables. Besides our regression-based method, there has another naive method to compute the CMs by using the ECQs as well. Let $I(\cdot)$ be the indicator function. The idea of this naive

method is straightforward, since it simply constructs a step distribution function $F_t^*(x)$ to approximate the conditional distribution of y_t , where

$$(2.12) \quad F_t^*(x) = \sum_{i=0}^n \alpha_i^* \mathbf{I}(Q_t(\alpha_i) \leq x < Q_t(\alpha_{i+1}))$$

with $Q_t(\alpha_0) = -\infty$, $Q_t(\alpha_{n+1}) = \infty$, $\alpha_0^* = 0$, $\alpha_i^* = (\alpha_i + \alpha_{i+1})/2$ for $i = 1, \dots, n-1$, and $\alpha_n^* = 1$. Here, the quantile levels α_i , $i = 1, \dots, n$, are different in (2.12). As $F_t^*(x)$ is a step distribution function, we can easily compute the explicit formulas of its mean, variance, skewness, and kurtosis as follows:

$$\begin{aligned} \mu_t^* &= \sum_{i=1}^n (\alpha_i^* - \alpha_{i-1}^*) Q_t(\alpha_i), & h_t^* &= \sum_{i=1}^n (\alpha_i^* - \alpha_{i-1}^*) [Q_t(\alpha_i) - \mu_t^*]^2, \\ s_t^* &= \sum_{i=1}^n (\alpha_i^* - \alpha_{i-1}^*) \left[\frac{Q_t(\alpha_i) - \mu_t^*}{\sqrt{h_t^*}} \right]^3, & k_t^* &= \sum_{i=1}^n (\alpha_i^* - \alpha_{i-1}^*) \left[\frac{Q_t(\alpha_i) - \mu_t^*}{\sqrt{h_t^*}} \right]^4, \end{aligned}$$

which can be estimated by $\hat{\mu}_t^*$, \hat{h}_t^* , \hat{s}_t^* , and \hat{k}_t^* , respectively, with $Q_t(\alpha_i)$ replaced by $\hat{Q}_t(\alpha_i)$. Because the conditional distribution of y_t is approximated by $F_t^*(x)$, it is thus rational to use the so-called naive QCMs $\hat{\mu}_t^*$, \hat{h}_t^* , \hat{s}_t^* , and \hat{k}_t^* to estimate four CMs μ_t , h_t , s_t , and k_t , respectively.

Note that a similar idea as the naive QCM has been adopted in [Sgouropoulos et al. \(2015\)](#) to propose the matching quantiles estimation for linear regression models. Although both naive QCM and our regression-based QCM methods aim to use the ECQs to estimate h_t , s_t , and k_t , they have two major differences. First, the regression-based QCM method can estimate h_t , s_t , and k_t simultaneously, whereas the naive QCM method has to do it sequentially. It turns out that the sequential estimation in the naive QCM method has the drawback to amplify the approximation errors (by using $\hat{Q}_t(\alpha_i)$ to replace $Q_t(\alpha_i)$) stepwisely, so that \hat{h}_t^* , \hat{s}_t^* , and \hat{k}_t^* are more sensitive to the choices of $\hat{Q}_t(\alpha_i)$ than \hat{h}_t , \hat{s}_t , and \hat{k}_t , respectively (see the numerical evidences in Section 5 below). Second, the regression-based QCM method can easily pool different ECQs at a given quantile level into the regression model (2.6), whereas the naive QCM method can only use one of ECQs (or the averaged ECQs) at a given quantile level. As

a result, the regression-based QCM method can have a larger effective sample size than the naive QCM method at each timepoint, leading to a more effective estimation of h_t , s_t , and k_t .

3. Asymptotics. This section studies the asymptotics of \hat{h}_t , \hat{s}_t , and \hat{k}_t at a fixed timepoint t . Let \xrightarrow{p} denote convergence in probability. To derive the consistency of \hat{h}_t , \hat{s}_t , and \hat{k}_t in (2.8), the following assumptions are needed.

ASSUMPTION 3.1. $\mathbf{M}_n \equiv \mathbf{Z}'\mathbf{Z}/n$ is uniformly positive definite.

ASSUMPTION 3.2. $\mathbf{Z}'\boldsymbol{\varepsilon}_t/n \xrightarrow{p} \mathbf{0}$ as $n \rightarrow \infty$.

We offer some remarks on the aforementioned assumptions. Assumption 3.1 is regular for linear regression models, and it holds as long as \mathbf{Z} is fully ranked (i.e., $\text{Rank}(\mathbf{Z})=4$). Because $\varepsilon_{t,i} = \varepsilon_{t,i}^* + \varepsilon_{t,i}^\circ - \gamma_t$, Assumption 3.2 is equivalent to

$$(3.1) \quad C_{t,*} + C_{t,\circ} - C_{t,\gamma} \xrightarrow{p} \mathbf{0} \text{ as } n \rightarrow \infty,$$

where $C_{t,*} = n^{-1} \sum_{i=1}^n \mathbf{Z}_i \varepsilon_{t,i}^*$, $C_{t,\circ} = n^{-1} \sum_{i=1}^n \mathbf{Z}_i \varepsilon_{t,i}^\circ$, and $C_{t,\gamma} = (n^{-1} \sum_{i=1}^n \mathbf{Z}_i) \gamma_t$. By law of large numbers for dependent and heteroscedastic data sequence (Andrews, 1988), it is reasonable to assert that $C_{t,*} = n^{-1} \sum_{i=1}^n \mathbf{Z}_i E(\varepsilon_{t,i}^*) + o_p(1)$ and $C_{t,\circ} = n^{-1} \sum_{i=1}^n \mathbf{Z}_i E(\varepsilon_{t,i}^\circ) + o_p(1)$. Then, since $\varepsilon_{t,i}^\bullet = \varepsilon_{t,i}^* + \varepsilon_{t,i}^\circ$, condition (3.1) holds if

$$(3.2) \quad \frac{1}{n} \sum_{i=1}^n \mathbf{Z}_i [E(\varepsilon_{t,i}^\bullet) - \gamma_t] \longrightarrow \mathbf{0} \text{ as } n \rightarrow \infty.$$

Condition (3.2) reveals an important fact that the role of γ_t is to offset the possible non-identification effect caused by the non-zero mean of $\varepsilon_{t,i}^\bullet$. In other words, to achieve the identification, γ_t should automatically tend to minimize the absolute difference

$$d_{n,t} \equiv \left| \frac{1}{n} \sum_{i=1}^n \mathbf{Z}_i [E(\varepsilon_{t,i}^\bullet)] - \left(\frac{1}{n} \sum_{i=1}^n \mathbf{Z}_i \right) \gamma_t \right|$$

for large n . Clearly, if $d_{n,t} \approx 0$ for large n , Condition (3.2) holds automatically, so then Assumption 3.2 most likely holds.

Next, we study the behavior of $d_{n,t}$ in different cases. For the first case that $E(\varepsilon_{t,i}^\bullet) \approx c_t$ for all i , we have $d_{n,t} \approx 0$ with $\gamma_t = c_t$. For the second case that $E(\varepsilon_{t,i}^\bullet) \approx 0$ for most of i , we also have $d_{n,t} \approx 0$ with $\gamma_t = 0$. For the third case that $n^{-1} \sum_{i=1}^n \mathbf{Z}_i [E(\varepsilon_{t,i}^\bullet)] \approx \boldsymbol{\tau}_t \approx \mathbf{z} f_t$ and $n^{-1} \sum_{i=1}^n \mathbf{Z}_i \approx \mathbf{z}$ for large n , we again have $d_{n,t} \approx 0$ with $\gamma_t = f_t$. For other cases, we still have the chance to ensure $d_{n,t} \approx 0$, depending on the behavior of $E(\varepsilon_{t,i}^\bullet)$ across i . In summary, the condition that $E(\varepsilon_{t,i}^\bullet) \approx 0$ for all i is not necessary for the validity of Assumption 3.2. Note that $\varepsilon_{t,i}^*$ usually has a negligible effect on the QCMs as shown by our simulation studies below. This implies that Assumption 3.2 allows $E(\varepsilon_{t,i}^\circ)$ to have the large non-zero absolute values across i (that is, the large biases of ECQs caused by the use of mis-specified conditional quantile models).

The following theorem establishes the consistency of \hat{h}_t , \hat{s}_t , and \hat{k}_t .

THEOREM 3.1. *Suppose that Assumptions 3.1–3.2 hold. Then, $\hat{\boldsymbol{\theta}}_t - \boldsymbol{\theta}_t \xrightarrow{p} 0$ as $n \rightarrow \infty$. Consequently, $\hat{h}_t - h_t \xrightarrow{p} 0$, $\hat{s}_t - s_t \xrightarrow{p} 0$, and $\hat{k}_t - k_t \xrightarrow{p} 0$ as $n \rightarrow \infty$.*

REMARK 3.1. *If we assume $\mathbf{Z}'\boldsymbol{\varepsilon}_t/n \rightarrow \mathbf{0}$ almost surely as $n \rightarrow \infty$ in Assumption 3.2, all of convergence results in Theorem 3.1 hold almost surely.*

REMARK 3.2. *In Theorem 3.1, we require large n but not large T . Certainly, a large T may improve the performance of ECQs with small biases, however, it is not necessary for the validity of Assumption 3.2 and thus the consistency of QCMs.*

Let \xrightarrow{d} denote convergence in distribution. We raise the following higher order assumption to replace Assumption 3.2:

ASSUMPTION 3.3. $[\mathbf{V}_{t,n}]^{-1/2} [\mathbf{Z}'\boldsymbol{\varepsilon}_t/\sqrt{n}] \xrightarrow{d} N(0, \mathbf{I})$ as $n \rightarrow \infty$, where \mathbf{I} is an identity matrix, and $\mathbf{V}_{t,n} \equiv \text{var}(\mathbf{Z}'\boldsymbol{\varepsilon}_t/\sqrt{n})$ is bounded and uniformly positive definite.

Assumption 3.3 is regular for proving the asymptotic normality of OLS estimator (see White (2001)). The theorem below shows that \hat{h}_t , \hat{s}_t , and \hat{k}_t are \sqrt{n} -consistent but not asymptotically normal.

THEOREM 3.2. *Suppose that Assumptions 3.1 and 3.3 hold. Then,*

$$(\mathbf{M}_n^{-1} \mathbf{V}_{t,n} \mathbf{M}_n^{-1})^{-1/2} \sqrt{n}(\hat{\boldsymbol{\theta}}_t - \boldsymbol{\theta}_t) \xrightarrow{d} N(0, \mathbf{I})$$

as $n \rightarrow \infty$. Moreover, $\sqrt{n}(\hat{h}_t - h_t) = O_p(1)$, $\sqrt{n}(\hat{s}_t - s_t) = O_p(1)$, and $\sqrt{n}(\hat{k}_t - k_t) = O_p(1)$, but \hat{h}_t , \hat{s}_t , and \hat{k}_t are not asymptotically normal.

REMARK 3.3. *Although \hat{h}_t , \hat{s}_t , and \hat{k}_t are not asymptotically normal, the asymptotic normality of $\hat{\boldsymbol{\theta}}_t$ demonstrates that the quantiled volatility (the second entry of $\hat{\boldsymbol{\theta}}_t$), denoted by $\hat{\sigma}_t$, has the asymptotic normality property: $(\mathbf{\Gamma} \mathbf{M}_n^{-1} \mathbf{V}_{t,n} \mathbf{M}_n^{-1} \mathbf{\Gamma}')^{-1/2} \sqrt{n}(\hat{\sigma}_t - \sigma_t) \xrightarrow{d} N(0, 1)$ as $n \rightarrow \infty$, where $\mathbf{\Gamma} = (0, 1, 0, 0)$.*

As shown before, the asymptotics of QCMs in Theorems 3.1–3.2 hold with no need to consider the specification of conditional mean and choose the specifications of conditional quantiles correctly. This important feature guarantees that the QCM method can largely reduce the risk of model mis-specification. The reason of this feature is that the QCM method is regression-based. Specifically, the conditional mean μ_t is absorbed into the intercept parameter $\beta_{0,t}$, so that it has no impact on the QCMs; meanwhile, the biases of ECQs from the use of wrongly specified conditional quantile models can be aggregately offset by the term γ_t , which is also nested in $\beta_{0,t}$.

The only price of the above feature is that we need to estimate conditional quantiles n different times. Fortunately, this seems a small and acceptable price, since the quantile estimation commonly can be computed easily by the linear programming method and the resulting estimation biases can be tolerated by the QCM method to a large extent.

4. Practical Implementations. To compute three QCMs in (2.8), we only need to input n different ECQs $\widehat{Q}_t(\alpha_i)$, which can be computed in many different ways; see, for example, McNeil and Frey (2000), Kuester et al. (2006), Xiao and Koenker (2009) and the references therein for earlier works, and Koenker et al. (2017) and Zheng et al. (2018) for more recent ones. Without assuming any parametric specifications of CMs, Engle and Manganelli (2004) propose a general class of CAViaR models, which can decently specify the dynamic specification of conditional quantiles. Hence, the CAViaR models are appropriate choices for us to compute $\widehat{Q}_t(\alpha_i)$. Following Engle and Manganelli (2004), we consider four CAViaR models below:

- (1) *Symmetric Absolute Value (SAV) model*: $Q_t(\alpha) = \psi_{1,0} + \psi_{2,0}Q_{t-1}(\alpha) + \psi_{3,0}|y_{t-1}|$;
- (2) *Asymmetric Slope (AS) model*: $Q_t(\alpha) = \psi_{1,0} + \psi_{2,0}Q_{t-1}(\alpha) + \psi_{3,0}(y_{t-1})^+ + \psi_{4,0}(y_{t-1})^-$,
where $(y_{t-1})^+ = \max(y_{t-1}, 0)$ and $(y_{t-1})^- = \min(y_{t-1}, 0)$;
- (3) *Indirect GARCH (IG) model*: $Q_t(\alpha) = (\psi_{1,0} + \psi_{2,0}Q_{t-1}^2(\alpha) + \psi_{3,0}y_{t-1}^2)^{1/2}$;
- (4) *Adaptive (ADAP) model*: $Q_t(\alpha) = Q_{t-1}(\alpha) + \psi_{1,0}\{[1 + \exp(N[y_{t-1} - Q_{t-1}(\alpha)])]^{-1} - \alpha\}$,
where N is a positive finite number.

Each CAViaR model above can be estimated via the classical quantile estimation method (Koenker and Bassett, 1978). For simplicity, we take the SAV model as an illustrating example. Let $\boldsymbol{\psi} = (\psi_1, \psi_2, \psi_3)'$ be the unknown parameter of SAV model, and $\boldsymbol{\psi}_0 = (\psi_{1,0}, \psi_{2,0}, \psi_{3,0})'$ be its true value. As in Engle and Manganelli (2004), we estimate $\boldsymbol{\psi}_0$ by the quantile estimator $\widehat{\boldsymbol{\psi}}_n \equiv \arg \min_{\boldsymbol{\psi}} \rho_{\alpha}(y_t - Q_t(\alpha, \boldsymbol{\psi}))$, where $\rho_{\alpha}(x) = x[\alpha - I(x < 0)]$ is the check function, and $Q_t(\alpha, \boldsymbol{\psi})$ is defined in the same way as $Q_t(\alpha)$ in the SAV model with $\boldsymbol{\psi}_0$ replaced by $\boldsymbol{\psi}$. Once $\widehat{\boldsymbol{\psi}}_n$ is obtained, we then take $\widehat{Q}_t(\alpha) \equiv Q_t(\alpha, \widehat{\boldsymbol{\psi}}_n)$ as our ECQ.

Using the above CAViaR models, we can obtain different $\widehat{Q}_t(\alpha)$. However, at some quantile levels α , some of models may be inadequate to specify the dynamic structure of $Q_t(\alpha)$, resulting in invalid $\widehat{Q}_t(\alpha)$. To screen out those invalid $\widehat{Q}_t(\alpha)$ before computing the QCMs, we consider the in-sample dynamic quantile (DQ) test $DQ_{IS}(\alpha)$ in Section 6 of Engle and Manganelli (2004). This test $DQ_{IS}(\alpha)$ aims to detect the inadequacy of CAViaR models by examining

whether $\bar{\mathbf{X}}_t(\alpha)\text{Hit}_t(\alpha)$ has mean zero, where $\text{Hit}_t(\alpha) \equiv \mathbf{I}(y_t < Q_t(\alpha)) - \alpha$ and $\bar{\mathbf{X}}_t(\alpha) \equiv (\text{Hit}_{t-1}(\alpha), \dots, \text{Hit}_{t-4}(\alpha))'$. The testing idea of $\text{DQ}_{IS}(\alpha)$ relies on the fact that $\bar{\mathbf{X}}_t(\alpha)\text{Hit}_t(\alpha)$ has mean zero when the CAViaR model specifies the dynamic structure of $Q_t(\alpha)$ correctly. Based on the sequence $\{\hat{Q}_t(\alpha)\}_{t=1}^T$ from a given CAViaR model, we can compute $\text{DQ}_{IS}(\alpha)$ and then its p-value $P(\xi > \text{DQ}_{IS}(\alpha))$, where $\xi \sim \chi_4^2$ (a Chi-squared distribution with 4 degrees of freedom). If the p-value of $\text{DQ}_{IS}(\alpha)$ is less than p^* , the corresponding ECQs $\{\hat{Q}_t(\alpha)\}$ are deemed to be invalid, so they are not included to compute the QCMs.

Below, we summarize our aforementioned procedure to compute the QCMs:

Procedure 4.1. (The steps to compute \hat{h}_t , \hat{s}_t , and \hat{k}_t)

1. Obtain $\{\hat{Q}_t(\alpha)\}_{t=1}^T$ at any quantile level α in $\boldsymbol{\alpha}$ based on any CAViaR model in \mathcal{M} , where $\boldsymbol{\alpha} \equiv [0.01 : 0.01 : 0.99]$ is a sequence of real numbers from 0.01 to 0.99 incrementing by 0.01, and $\mathcal{M} \equiv \{\text{SAV}, \text{AS}, \text{IG}, \text{ADAP}\}$.
2. Apply the DQ test $\text{DQ}_{IS}(\alpha)$ to each $\{\hat{Q}_t(\alpha)\}_{t=1}^T$ from Step 1, and discard those $\{\hat{Q}_t(\alpha)\}_{t=1}^T$ with p-values of $\text{DQ}_{IS}(\alpha)$ less than p^* .
3. Group all remaining $\hat{Q}_t(\alpha)$ to form a set \mathbf{S}_t at each given t . Then, take the i -th entry of \mathbf{S}_t to be $Y_{t,i}$ in (2.6), and use its corresponding quantile level to compute \mathbf{X}_i in (2.6), where $i = 1, \dots, n_0$, and n_0 is the size of \mathbf{S}_t .
4. Based on $\{Y_{t,i}, \mathbf{X}_i\}_{i=1}^{n_0}$ from Step 3, compute the OLS estimator $\hat{\boldsymbol{\theta}}_t$ in (2.7) and then the three QCMs \hat{h}_t , \hat{s}_t , and \hat{k}_t in (2.8).

In Procedure 4.1, the value of n_0 decreases with that of p^* , and it achieves the upper bound $n = 99 \times 4$ when $p^* = 0$ (i.e., no ECQs are discarded). Clearly, the choice of p^* reveals a trade-off between estimation reliability and estimation efficiency in the QCM method, since a large value of p^* enhances the reliability of $\hat{Q}_t(\alpha)$, but meanwhile, it reduces the efficiency of $\hat{\boldsymbol{\theta}}_t$ as the value of n_0 becomes small. So far, how to choose p^* optimally is unclear. Our additional simulation results in the supplementary materials show that $p^* = 0.1$ is a good choice to

balance the bias and variance of the estimation error of the QCMs. Hence, we recommend to take $p^* = 0.1$ for the practical use.

5. Simulations. This section examines the finite sample performance of three QCMs \hat{h}_t , \hat{s}_t , and \hat{k}_t with respect to the choice of $\hat{Q}_t(\alpha_i)$. For saving the space, some additional simulation results on the standard GARCH model and the selection of p^* are reported in the supplementary materials.

5.1. *Simulation settings.* Let $MN(\lambda_1, \lambda_2, \tau_1, \tau_2, \sigma_1^2, \sigma_2^2)$ denote a mixed normal (MN) distribution, the density of which is a mixture of two normal densities of $N(\tau_1, \sigma_1^2)$ and $N(\tau_2, \sigma_2^2)$ with the weighting probabilities λ_1 and λ_2 , respectively, where $\lambda_i \in (0, 1)$, $i = 1, 2$, and $\lambda_1 + \lambda_2 = 1$. We generate 100 replications of sample size $T = 1000$ from the following ARMA–MN–GARCH model ([Haas et al., 2004](#))

$$(5.1) \quad y_t = a_0 + a_1 y_{t-1} + \epsilon_t + b_1 \epsilon_{t-1},$$

where $\epsilon_t \sim MN(\lambda_1, \lambda_2, \tau_1, \tau_2, \sigma_{1,t}^2, \sigma_{2,t}^2)$ with $\tau_2 = -(\lambda_1/\lambda_2)\tau_1$, $\sigma_{1,t}^2 = c_{10} + c_{11}\epsilon_{t-1}^2 + c_{12}\sigma_{1,t-1}^2$, and $\sigma_{2,t}^2 = c_{20} + c_{21}\epsilon_{t-1}^2 + c_{22}\sigma_{2,t-1}^2$, and the parameters are chosen as $\lambda_1 = 0.2$, $\tau_1 = 0.4$, $a_0 = 0.5$, $a_1 = 0.4$, $b_1 = -0.3$, $c_{10} = 0.1$, $c_{20} = 0.3$, $c_{11} = 0.05$, $c_{21} = 0.1$, $c_{12} = 0.85$, and $c_{22} = 0.8$.

For each replication, we first compute the true values of CMs and conditional quantiles of y_t in model (5.1) as follows:

$$(5.2) \quad \begin{aligned} \mu_t &= a_0 + a_1 y_{t-1} + b_1 \epsilon_{t-1}, \\ h_t &= \lambda_1(\tau_1^2 + \sigma_{1,t}^2) + \lambda_2(\tau_2^2 + \sigma_{2,t}^2) - (\lambda_1 \tau_1 + \lambda_2 \tau_2)^2, \\ s_t &= \frac{\lambda_1(\tau_1^3 + 3\tau_1 \sigma_{1,t}^2) + \lambda_2(\tau_2^3 + 3\tau_2 \sigma_{2,t}^2)}{[\lambda_1(\tau_1^2 + \sigma_{1,t}^2) + \lambda_2(\tau_2^2 + \sigma_{2,t}^2)]^{3/2}}, \\ k_t &= \frac{\lambda_1(\tau_1^4 + 6\tau_1^2 \sigma_{1,t}^2 + 3\sigma_{1,t}^4) + \lambda_2(\tau_2^4 + 6\tau_2^2 \sigma_{2,t}^2 + 3\sigma_{2,t}^4)}{[\lambda_1(\tau_1^2 + \sigma_{1,t}^2) + \lambda_2(\tau_2^2 + \sigma_{2,t}^2)]^2}, \end{aligned}$$

and

$$(5.3) \quad Q_t(\alpha) = \mu_t + Q_t^\epsilon(\alpha),$$

where $Q_t^\epsilon(\alpha)$ satisfies $\lambda_1\Phi(Q_t^\epsilon(\alpha); \tau_1, \sigma_{1,t}^2) + \lambda_2\Phi(Q_t^\epsilon(\alpha); \tau_2, \sigma_{2,t}^2) = \alpha$, and $\Phi(x; \tau, \sigma^2)$ represents the normal distribution function with mean τ and variance σ^2 .

Next, we generate the sequence $\{\widehat{Q}_t(\alpha_i)\}$ at each t to compute \widehat{h}_t , \widehat{s}_t , and \widehat{k}_t in four different cases:

$$\begin{aligned}
 (5.4) \quad & \text{Case 1 [No Error]: } \widehat{Q}_t(\alpha_i) = Q_t(\alpha_i); \\
 & \text{Case 2 [Error I]: } \widehat{Q}_t(\alpha_i) = Q_t(\alpha_i) + \varepsilon_{t,i}^\circ \text{ with } \varepsilon_{t,i}^\circ \sim N(0, \sigma^2(\alpha_i)); \\
 & \text{Case 3 [Error II]: } \widehat{Q}_t(\alpha_i) = Q_t(\alpha_i) + \varepsilon_{t,i}^\circ \text{ with } \varepsilon_{t,i}^\circ \sim N(\mu(\alpha_i), \sigma^2(\alpha_i)); \\
 & \text{Case 4 [CAViaR]: } \widehat{Q}_t(\alpha_i) \text{ is the entry of } \mathbf{S}_t,
 \end{aligned}$$

where $\alpha_i \in \boldsymbol{\alpha}$ in Cases 1–3, $\boldsymbol{\alpha}$ and \mathbf{S}_t are defined as in Procedure 4.1, $Q_t(\alpha)$ is defined as in (5.3), $\sigma^2(\alpha) = 0.5\sigma^2 + |\alpha - 0.5|\sigma^2$ with $\sigma^2 = 0.2$, and $\mu(\alpha) = \exp(-200\alpha)\mathbf{I}(\alpha < 0.5) + \exp(-(2 - 200\alpha))\mathbf{I}(\alpha \geq 0.5)$.

Under the setting in Case 1, there has only expansion errors $\varepsilon_{t,i}^*$ but no approximation errors $\varepsilon_{t,i}^\circ$ in regression model (2.6). Under the settings in Cases 2 and 3, the approximation errors $\varepsilon_{t,i}^\circ$ are considered with different variances across α_i , where their means are zeros (Case 2) or non-zero values (Case 3) to mimic the scenario that $\widehat{Q}_t(\alpha_i)$ is an unbiased or biased estimator of $Q_t(\alpha_i)$, respectively. Under the setting in Case 4, $\widehat{Q}_t(\alpha_i)$ are computed by the CAViaR models, and this case mimics the real application scenario that the dynamic structures of $Q_t(\alpha_i)$ are unknown and modelled by the CAViaR models.

5.2. Performance of QCMs. Based on $\{\widehat{Q}_t(\alpha_i)\}$ generated by (5.4), we compute three QCMs \widehat{h}_t , \widehat{s}_t , and \widehat{k}_t for each replication, and then we measure their precision at each t by considering

$$(5.5) \quad \Delta_{h,t} = \widehat{h}_t - h_t, \quad \Delta_{s,t} = \widehat{s}_t - s_t, \quad \Delta_{k,t} = \widehat{k}_t - k_t,$$

where h_t , s_t , and k_t are the true values of three CMs defined as in (5.2). As a comparison, we also compute the naive QCMs \widehat{h}_t^* , \widehat{s}_t^* , and \widehat{k}_t^* in Section 2.4 and similarly measure their

precision at each t by considering

$$(5.6) \quad \Delta_{h,t}^* = \widehat{h}_t^* - h_t, \quad \Delta_{s,t}^* = \widehat{s}_t^* - s_t, \quad \Delta_{k,t}^* = \widehat{k}_t^* - k_t.$$

Note that if we have multiple valid $\widehat{Q}_t(\alpha_i)$ at a fixed quantile level α_i in Case 4, we average all of those valid $\widehat{Q}_t(\alpha_i)$ to calculate \widehat{h}_t^* , \widehat{s}_t^* , and \widehat{k}_t^* .

Based on the results of 100 replications, Figure 1 exhibits the boxplots of $\Delta_{h,t}$, $\Delta_{s,t}$, $\Delta_{k,t}$, $\Delta_{h,t}^*$, $\Delta_{s,t}^*$, and $\Delta_{k,t}^*$ for $t = 1, \dots, 10$ under four different cases in (5.4). The corresponding boxplots for $t \geq 11$ are similar and they thus are not reported here to make the figure more visible. From Figure 1, our findings are as follows:

1. When there has no approximation errors as in Case 1, the QCMs \widehat{h}_t , \widehat{s}_t , and \widehat{k}_t are very accurate estimators of h_t , s_t , and k_t , respectively. This indicates that the expansion errors in the QCM method have a negligible effect on the performance of \widehat{h}_t , \widehat{s}_t , and \widehat{k}_t . However, the naive QCMs \widehat{h}_t^* , \widehat{s}_t^* , and \widehat{k}_t^* have large biases in this case, and their bad performance is most likely due to its sequential estimation framework that reduces the estimation precision stepwisely.
2. When there has approximation errors with zero means (or nonzero means) as in Case 2 (or Case 3), the median lines in the boxplots of $\Delta_{h,t}$, $\Delta_{s,t}$, and $\Delta_{k,t}$ are generally close to zero, although $\Delta_{h,t}$, $\Delta_{s,t}$, and $\Delta_{k,t}$ in Case 3 exhibit slightly larger dispersion than Case 2. These results suggest that \widehat{h}_t , \widehat{s}_t , and \widehat{k}_t can still be the consistent estimators of h_t , s_t , and k_t , even when $\widehat{Q}_t(\alpha_i)$ are biased estimators of $Q_t(\alpha_i)$. On the contrary, the median lines in the boxplots of $\Delta_{h,t}^*$, $\Delta_{s,t}^*$, and $\Delta_{k,t}^*$ demonstrate that \widehat{h}_t^* , \widehat{s}_t^* , and \widehat{k}_t^* are inconsistent in Cases 2 and 3, since they are still biased estimators as in Case 1.
3. When $\widehat{Q}_t(\alpha_i)$ are estimated by using the CAViaR method as in Case 4, the boxplots of $\Delta_{h,t}$, $\Delta_{s,t}$, and $\Delta_{k,t}$ show similar patterns as those in Case 2. Hence, the consistency of \widehat{h}_t , \widehat{s}_t , and \widehat{k}_t still hold, though the dynamic structures of $Q_t(\alpha_i)$ are mis-specified by the CAViaR models. This finding implies that $\widehat{Q}_t(\alpha_i)$ is very likely still the consistent

estimator of $Q_t(\alpha_i)$ in the mis-specified case. For \hat{h}_t^* , \hat{s}_t^* , and \hat{k}_t^* , they have the worst performance in this mis-specified case, showing that the naive QCMs are much more sensitive to the choices of $\hat{Q}_t(\alpha_i)$ than the QCMs.

6. A Real Application. In our empirical work, we consider the log-return (in percentage) series of eight major stock indexes, including the Standard and Poor’s 500 (S&P500), Nasdaq Composite (NAS), Dow Jones Industrial Average (DJIA), and Russell 2000 (R2000) from the U.S., the STOXX Europe 600 (SXXP) and Financial Times Stock Exchange 100 (FTSE) from Europe, and the Nikkei 225 (N225) and Hang Seng (HS) from Asia. We denote each log-return series by $\{y_1, \dots, y_T\}$, which are computed from the index data from January 1, 2009 to December 31, 2021. See Table 1 for some basic descriptive statistics of all eight log-return series. Below, we compute the three QCMs of each log-return series, and then use these QCMs to study the “News impact curve” (NIC).

TABLE 1
Descriptive statistics for eight return series.

	S&P500	NAS	DJI	R2000	SXXP	FTSE	N225	HSI
Sample size	3272	3272	3274	3272	3382	3379	3179	3206
Sample mean	0.0499	0.0691	0.0425	0.0455	0.0266	0.0151	0.0364	0.0138
Sample variance	1.3118	1.6216	1.2468	2.2881	1.2132	1.1170	1.8585	1.6103
Sample skewness	−0.6834	−0.6095	−0.7698	−0.6841	−0.7093	−0.5803	−0.3767	−0.1628
Sample kurtosis	16.1831	11.7659	21.2789	12.0976	11.8995	11.7389	7.5532	5.2568

6.1. *The three QCMs of return series.* Following the steps in Procedure 4.1, we compute the three QCMs \hat{h}_t , \hat{s}_t , and \hat{k}_t of each log-return series, and report their basic descriptive statistics in Table 2, where the constraint (2.11) holds for all of the computed QCMs. From Tables 1 and 2, we find that for each return series, the mean of \hat{h}_t (or \hat{s}_t) is close to the corresponding sample variance (or skewness), whereas the mean of \hat{k}_t is much smaller than the corresponding sample

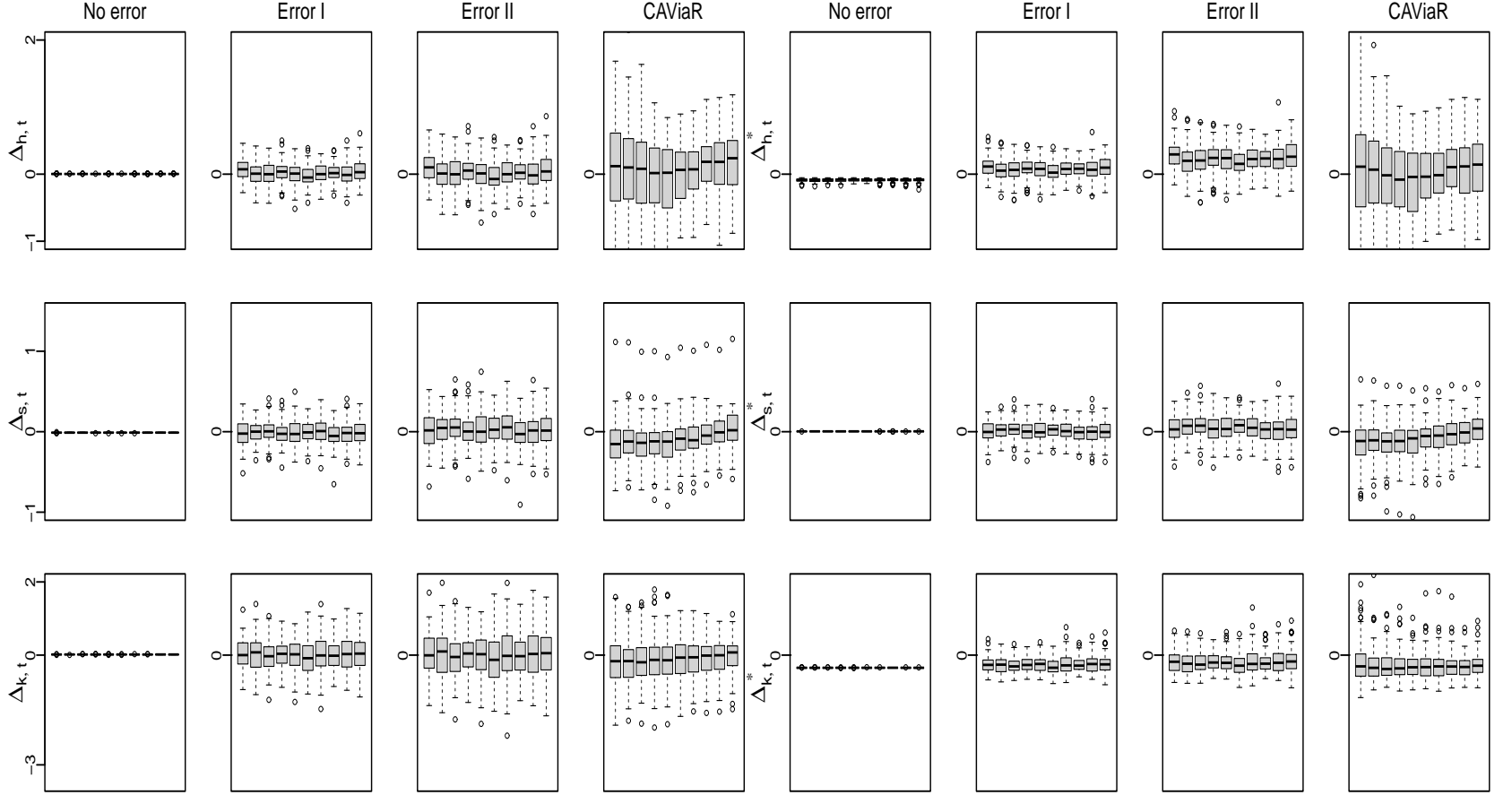


Fig 1: The boxplots of $\Delta_{h,t}$, $\Delta_{s,t}$, $\Delta_{k,t}$, $\Delta_{h,t}^*$, $\Delta_{s,t}^*$, and $\Delta_{k,t}^*$ for $t = 1, \dots, 10$ under four different cases in (5.4), where the data are generated from the ARMA-MN-GARCH model in (5.1). In each boxplot, the lines from top to bottom represent the maximum, first quartile, median, third quartile, and maximum of the data, and the outliers are plotted individually using the 'o' marker symbol.

kurtosis. These findings are expected, since extreme returns can affect the sample kurtosis for a prolonged period of time, but their impact on \hat{k}_t decays exponentially over time.

TABLE 2
Descriptive statistics for the three QCMs of eight return series.

		S&P500	NAS	DJIA	R2000	SXXP	FTSE	N225	HS
\hat{h}_t	Mean	1.2627	1.6094	1.2163	2.1899	1.1986	1.1131	1.8357	1.6171
	Maximum	36.2215	34.5558	51.6933	46.2633	16.9105	13.4815	17.3361	6.6813
	Minimum	0.1432	0.2747	0.1494	0.3167	0.1867	0.2142	0.4718	0.4273
	Ljung-Box [†]	0.0000	0.0000	0.0000	0.0000	0.0000	0.0000	0.0000	0.0000
\hat{s}_t	Mean	-0.4953	-0.4713	-0.3924	-0.3637	-0.3349	-0.2721	-0.2894	-0.2388
	Maximum	0.0096	-0.0092	0.3171	0.1858	0.2139	0.3194	0.0908	0.2942
	Minimum	-1.1517	-0.9676	-1.2426	-1.0594	-0.9708	-1.2020	-0.6281	-0.8702
	Ljung-Box	0.0000	0.0000	0.0000	0.0000	0.0000	0.0000	0.0000	0.0000
\hat{k}_t	Mean	4.0190	4.1270	3.9847	3.4322	3.9933	4.0940	3.8377	3.9489
	Maximum	6.3107	6.2797	7.1529	5.6968	5.9212	6.2937	6.1539	5.2981
	Minimum	2.0846	2.6694	2.1669	1.6534	2.8413	2.7411	2.5785	2.9419
	Ljung-Box	0.0000	0.0000	0.0000	0.0000	0.0000	0.0000	0.0000	0.0000

[†] The results are the p-values of Ljung-Box test (Ljung and Box, 1978).

Next, we check the validity of QCMs via a similar method as in Gu et al. (2020). Denote $\alpha^h = E(e_t^h)$, $\alpha^s = E(e_t^s)$, and $\alpha^k = E(e_t^k)$, where $e_t^h = (y_t - \mu_t)^2 - h_t$, $e_t^s = [(y_t - \mu_t)/\sqrt{h_t}]^3 - s_t$, and $e_t^k = [(y_t - \mu_t)/\sqrt{h_t}]^4 - k_t$. Based on the estimates $\hat{e}_t^h = (y_t - \hat{\mu}_t)^2 - \hat{h}_t$, $\hat{e}_t^s = [(y_t - \hat{\mu}_t)/\sqrt{\hat{h}_t}]^3 - \hat{s}_t$, and $\hat{e}_t^k = [(y_t - \hat{\mu}_t)/\sqrt{\hat{h}_t}]^4 - \hat{k}_t$, we utilize the Student's t tests \mathbb{T}^h , \mathbb{T}^s , and \mathbb{T}^k to test the null hypotheses $\mathbb{H}^h: a^h = 0$, $\mathbb{H}^s: a^s = 0$, and $\mathbb{H}^k: a^k = 0$, respectively. Here, $\hat{\mu}_t$ is the estimate of conditional mean, and it is computed based on the mean specifications in Section 6.2 below. If \mathbb{H}^h is not rejected by \mathbb{T}^h at the significance level α^* , then it is reasonable to conclude that \hat{h}_t is valid. Similarly, the validity of \hat{s}_t and \hat{k}_t can be examined by using \mathbb{T}^s and \mathbb{T}^k . Table 3 reports the p-values of \mathbb{T}^h , \mathbb{T}^s , and \mathbb{T}^k for all eight markets, and the results imply that all QCMs are

valid at the significance level 5%.

TABLE 3
The p-values of T^h , T^s , and T^k for checking the validity of QCMs.

	S&P500	NAS	DJI	R2000	SXXP	FTSE	N225	HSI
T^h	0.6092	0.3950	0.2286	0.9654	0.8234	0.9511	0.7810	0.8940
T^s	0.0627	0.0650	0.0819	0.1744	0.1161	0.1438	0.2798	0.5906
T^k	0.4236	0.6205	0.6809	0.5248	0.7773	0.8980	0.3893	0.7784

After checking the validity of the QCMs, we further plot the QCMs of all eight return series during a sub-period from January 2, 2020 to May 1, 2020 in Figure 2. This sub-period deserves a detailed study, since it covers the 2020 stock market crash caused by the COVID-19 pandemic. For ease of visualization, the plots of all computed QCMs for the entire examined time period are not given here but available upon request. From Figure 2, we can have the following interesting findings:

1. Starting from February 20, there is a rapid rising trend for both \hat{h}_t and \hat{k}_t while an apparent decline trend for \hat{s}_t in all of examined stock markets, except for \hat{s}_t in the N225 stock market and \hat{k}_t in the HS stock market. These observed trends demonstrate that the volatility risk kept rising sharply in stock markets, and synchronically, the tail risk to have extremely negative returns kept increasing substantially to make things even worse. The above phenomenon is expected, since the U.S. stock market triggered several trading curbs in March 2020, leading to a worldwide financial crisis during that time. After March 17 or March 26, all of \hat{h}_t , \hat{s}_t , and \hat{k}_t exhibited opposite trends. This is very likely because the Federal Reserve and many central banks announced their financial rescue plans on March 17, and the G20 Summit did the similar things on March 26. Hence, the trend reversal sheds light on the effectiveness of the issued financial plans in rescuing stock markets.
2. The exception for \hat{s}_t having stable values from February 20 to March 17 in the N225

stock market is probably because the N225 index is well-known for its low value of price/earnings ratio. Therefore, the investors in the Japanese market could bear a bigger risk of price drop than those in other markets, resulting in a relatively more stable behavior of \hat{s}_t . Another exception was observed in the HS stock market for \hat{k}_t to have stable values from February 20 to March 26. One possible explanation for this observation is that the investment from China through Shanghai-Hong Kong Stock Connect helps to avoid extremely large volatilities in the HS stock market during that period.

Overall, we find that the COVID-19 pandemic has a perilous impact on the examined eight major stock markets, and the financial rescue plans are effective in reducing the values of conditional variance and kurtosis, while at the same time, increasing the values of conditional skewness, so creating a very good investment opportunity for investors to make profits.

6.2. *The study on NICs.* The NIC initiated by [Engle and Ng \(1993\)](#) aims to study how past shocks (or news) $\{\epsilon_i\}_{i \leq t-1}$ affect the present conditional variance h_t by assuming

$$(6.1) \quad h_t = \theta_h h_{t-1} + g_h(\epsilon_{t-1}),$$

where $\epsilon_t \equiv y_t - \mu_t$ is the collective shock at t , $\theta_h \in (0, 1)$ is an unknown parameter to measure the persistence of h_t , and $g_h(\cdot)$ is the NIC function for h_t that has a specific parametric form. For example, researchers commonly assume that

$$(6.2) \quad g_h(x) = \vartheta_{h,0} + \vartheta_{h,1}x^2,$$

$$(6.3) \quad g_h(x) = \vartheta_{h,0} + \vartheta_{h,1}x^2 + \vartheta_{h,2}x^2\mathbf{I}(x < 0),$$

where the specifications of $g_h(\cdot)$ in (6.2) and (6.3) lead to the standard GARCH ([Bollerslev, 1986](#)) and GJR-GARCH ([Glosten et al., 1993](#)) models for h_t , respectively. Similar to the NIC for h_t in (6.1), we can follow the ideas of [Harvey and Siddique \(1999\)](#) and [León et al. \(2005\)](#)

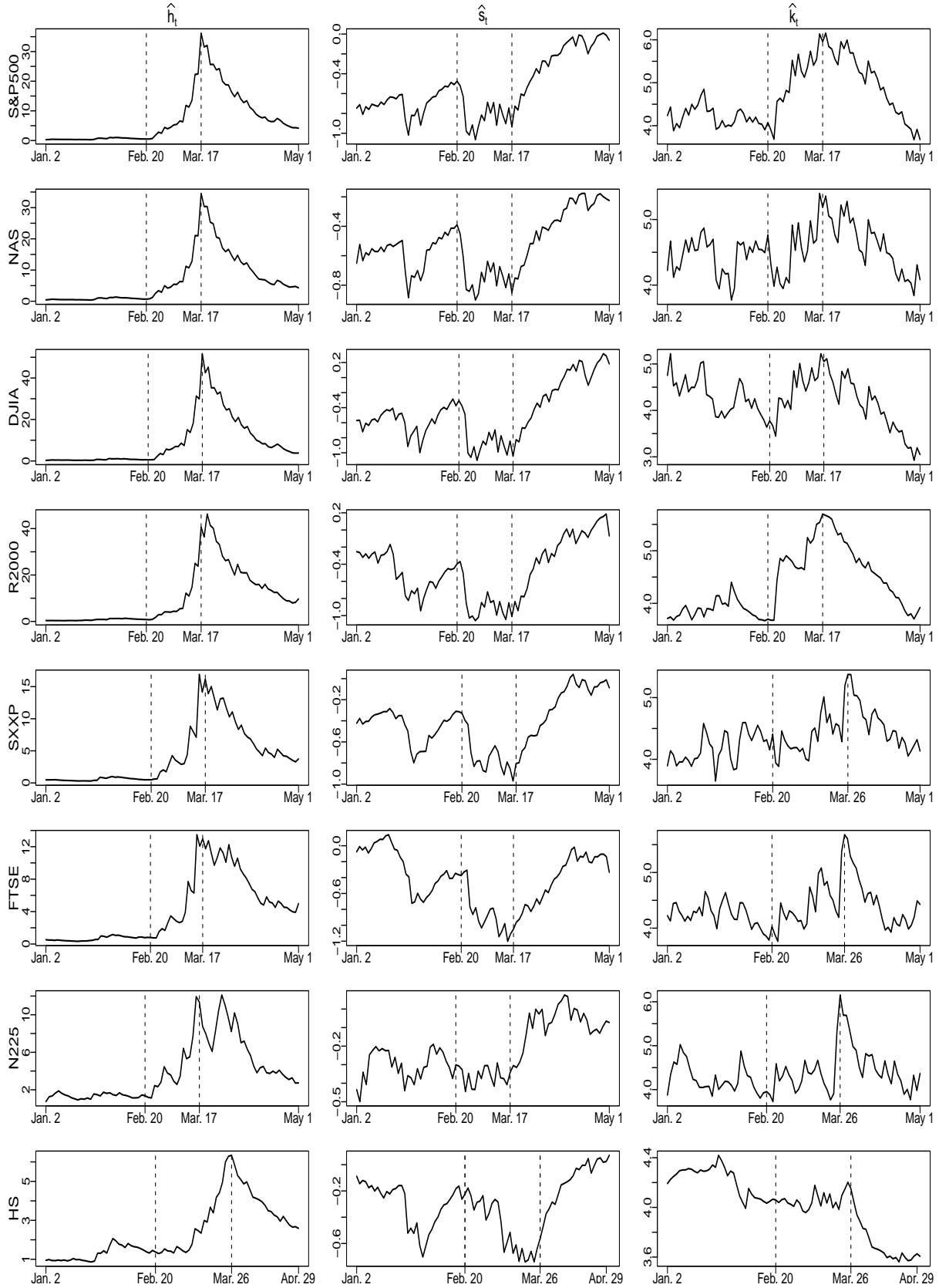


Fig 2: The plots of \hat{h}_t , \hat{s}_t , and \hat{k}_t of eight return series from January 2, 2020 to May 1, 2020.

to consider the NICs for s_t and k_t :

$$(6.4) \quad s_t = \theta_s s_{t-1} + g_s(\varrho_{t-1}),$$

$$(6.5) \quad k_t = \theta_k k_{t-1} + g_k(\varrho_{t-1}),$$

where $\varrho_t \equiv \epsilon_t / \sqrt{h_t}$ is the re-scaled collective shock at t , $\theta_s \in (-1, 1)$ and $\theta_k \in (0, 1)$ are two unknown parameters to measure the persistence of s_t and k_t , respectively, and $g_s(\cdot)$ and $g_k(\cdot)$ are the NIC functions for s_t and k_t , respectively. As for $g_h(\cdot)$, $g_s(\cdot)$ and $g_k(\cdot)$ are often assumed to have certain parametric forms, such as

$$(6.6) \quad g_s(x) = \vartheta_{s,0} + \vartheta_{s,1}x^3,$$

$$(6.7) \quad g_k(x) = \vartheta_{k,0} + \vartheta_{k,1}x^4;$$

see, for example, [Harvey and Siddique \(1999\)](#) and [León et al. \(2005\)](#). Since h_t , s_t , k_t , ϵ_t , and ϱ_t are generally unobserved, all of the unknown parameters in (6.1) and (6.4)–(6.5) have to be estimated by specifying some parametric models on y_t that account for the conditional variance, skewness, and kurtosis simultaneously.

However, so far the parametric forms of $g_h(\cdot)$, $g_s(\cdot)$, and $g_k(\cdot)$ are chosen in an ad-hoc rather than a data-driven manner. Intuitively, if $g_h(\cdot)$, $g_s(\cdot)$, and $g_k(\cdot)$ can be estimated non-parametrically, we are able to get some useful information on their parametric forms. Motivated by this idea, we replace h_t , s_t , k_t , ϵ_{t-1} , and ϱ_{t-1} in (6.1) and (6.4)–(6.5) with \hat{h}_t , \hat{s}_t , \hat{k}_t , $\hat{\epsilon}_{t-1}$, and $\hat{\varrho}_{t-1}$, respectively, where $\hat{\epsilon}_t = y_t - \hat{\mu}_t$ and $\hat{\varrho}_t = \hat{\epsilon}_t / \sqrt{\hat{h}_t}$ with $\hat{\mu}_t$ being an estimator of μ_t . After this replacement, we can get the following models:

$$(6.8) \quad \hat{h}_t = \theta_h \hat{h}_{t-1} + g_h(\hat{\epsilon}_{t-1}) + \varsigma_{h,t},$$

$$(6.9) \quad \hat{s}_t = \theta_s \hat{s}_{t-1} + g_s(\hat{\varrho}_{t-1}) + \varsigma_{s,t},$$

$$(6.10) \quad \hat{k}_t = \theta_k \hat{k}_{t-1} + g_k(\hat{\varrho}_{t-1}) + \varsigma_{k,t},$$

where $\varsigma_{h,t}$, $\varsigma_{s,t}$, and $\varsigma_{k,t}$ are model errors caused by the replacement. Since the QCMs are most likely consistent estimators of CMs, all model errors are expected to have desirable properties for valid model estimations when the parametric form of μ_t is correctly specified.

To get the correct specification of μ_t , we apply two Cramér-von Mises tests $D_{T,I}^2$ and $D_{T,C}^2$ in Escanciano (2006) to check whether the assumed form of μ_t is correctly specified, where the p-values of $D_{T,I}^2$ and $D_{T,C}^2$ are computed via the bootstrap method in Escanciano (2006). Since the strong autocorrelations are detected for the four return series in the U.S. market, we adopt an order p threshold autoregressive (TAR(p)) model (Tong, 1978) with threshold variable being zero and delay variable being one to fit these four return series. After dismissing insignificant parameters, the S&P500, NAS, and DJIA return series are fitted by the TAR(9) model, and the R2000 return series is fitted by the TAR(7) model. The p-values of $D_{T,I}^2$ and $D_{T,C}^2$ in Table 4 indicate that these TAR models are correct specifications for the four return series in the U.S. market at the significance level 5%. In contrast, since no strong autocorrelations are detected for other four return series in Europe and Asia, we fit these four series by a constant model. The related p-values of $D_{T,I}^2$ and $D_{T,C}^2$ in Table 4 imply that a constant model is the correct specification for the four return series in Europe and Asia at the significance level 5%.

TABLE 4
The p-values of $D_{T,I}^2$ and $D_{T,C}^2$ for checking the conditional mean specification.

	A TAR(p) model				A constant model			
	S&P500	NAS	DJIA	R2000	SXXP	FTSE	N225	HS
$D_{T,I}^2$	0.1880	0.1540	0.3040	0.1040	0.7020	0.8380	0.2860	0.4800
$D_{T,C}^2$	0.1960	0.1920	0.2600	0.1400	0.8980	0.9660	0.5000	0.7400

After estimating the chosen specifications of μ_t above by the least squares method, we are able to obtain $\hat{\epsilon}_{t-1}$ and \hat{q}_{t-1} . Define $K_b(\cdot) = K(\cdot/b)/b$, where $K(\cdot)$ is Gaussian kernel function and b is the bandwidth. Then, based on the sample sequence $\{(\hat{h}_t, \hat{h}_{t-1}, \hat{\epsilon}_{t-1})\}_{t=2}^T$, we use the

method in [Robinson \(1988\)](#) to estimate θ_h by

$$\hat{\theta}_h = \left\{ \sum_{t=2}^T [\hat{h}_{t-1} - \phi_1(\hat{\epsilon}_{t-1})]^2 \right\}^{-1} \left\{ \sum_{t=2}^T [\hat{h}_{t-1} - \phi_1(\hat{\epsilon}_{t-1})][\hat{h}_t - \phi_2(\hat{\epsilon}_{t-1})] \right\},$$

where

$$\phi_1(\cdot) = \frac{\sum_{s=2}^T K_{b_1}(\cdot - \hat{\epsilon}_{s-1})\hat{h}_{s-1}}{\sum_{s=2}^T K_{b_1}(\cdot - \hat{\epsilon}_{s-1})} \text{ and } \phi_2(\cdot) = \frac{\sum_{s=2}^T K_{b_2}(\cdot - \hat{\epsilon}_{s-1})\hat{h}_s}{\sum_{s=2}^T K_{b_2}(\cdot - \hat{\epsilon}_{s-1})},$$

and the values of b_1 and b_2 are chosen by the conventional cross-validation method. Next, we estimate $g_h(\cdot)$ non-parametrically by $\hat{g}_h(\cdot) = \sum_{s=2}^T K_{b_3}(\cdot - \hat{\epsilon}_{s-1})R_{h,s} / \sum_{s=2}^T K_{b_3}(\cdot - \hat{\epsilon}_{s-1})$, where $R_{h,t} = \hat{h}_t - \hat{\theta}_h \hat{h}_{t-1}$, and the value of b_3 is chosen by the cross-validation method. Similarly, based on the sample sequences $\{(\hat{s}_t, \hat{s}_{t-1}, \hat{\varrho}_{t-1})\}_{t=2}^T$ and $\{(\hat{k}_t, \hat{k}_{t-1}, \hat{\varrho}_{t-1})\}_{t=2}^T$, we estimate $g_s(\cdot)$ and $g_k(\cdot)$ non-parametrically by $\hat{g}_s(\cdot)$ and $\hat{g}_k(\cdot)$, respectively.

Figure 3 plots the non-parametric fitted models $\hat{g}_h(\cdot)$, $\hat{g}_s(\cdot)$, and $\hat{g}_k(\cdot)$ for all eight return series. From this figure, we find that the form of $g_h(\cdot)$ in (6.3) seems to match $\hat{g}_h(\cdot)$, whereas the forms of $g_s(\cdot)$ in (6.6) and $g_k(\cdot)$ in (6.7) exhibit a large deviation from $\hat{g}_s(\cdot)$ and $\hat{g}_k(\cdot)$, respectively, in many cases. Indeed, the plots of $\hat{g}_s(\cdot)$ and $\hat{g}_k(\cdot)$ in Figure 3 suggest the following parametric forms of $g_s(\cdot)$ and $g_k(\cdot)$:

$$(6.11) \quad g_s(x) = \vartheta_{s,0} + \vartheta_{s,1}x + \vartheta_{s,2}x\mathbf{I}(x < 0),$$

$$(6.12) \quad g_k(x) = \vartheta_{k,0} + \vartheta_{k,1}(x + \vartheta_{k,3})^2 + \vartheta_{k,2}(x + \vartheta_{k,3})^2\mathbf{I}(x + \vartheta_{k,3} < 0).$$

To compare the performance of NIC functions aforementioned, we estimate models (6.8)–(6.10) under different forms of $g_h(\cdot)$, $g_s(\cdot)$, and $g_k(\cdot)$, and plot the corresponding parametric fitted models in Figure 3. Here, the model related to $g_k(\cdot)$ in (6.12) is estimated by the least squares method for threshold models ([Chan, 1993](#)), whereas the other models are estimated by the least squares method for linear regression models. Table 5 reports the results of adjusted R^2 for all fitted models. From this table, we find that the form of $g_h(\cdot)$ in (6.3) only leads to a slightly better fitting than the one in (6.2), whereas the forms of $g_s(\cdot)$ in (6.11) and $g_k(\cdot)$ in

(6.12) give a much better fitting than their competitors in most of cases; see also the clear graphic evidence in Figure 3.

TABLE 5
The values of adjusted R^2 for the fitted models (6.8)–(6.10).

	S&P500	NAS	DJIA	R2000	SXXP	FTSE	N225	HS
Panel A: Model (6.8)								
$g_h(\cdot) \sim (6.2)$	0.9898	0.9889	0.9832	0.9880	0.9837	0.9902	0.9835	0.9964
$g_h(\cdot) \sim (6.3)$	0.9932	0.9940	0.9892	0.9927	0.9923	0.9946	0.9915	0.9979
Panel B: Model (6.9)								
$g_s(\cdot) \sim (6.6)$	0.8549	0.9265	0.8399	0.8730	0.9202	0.8894	0.7915	0.8898
$g_s(\cdot) \sim (6.11)$	0.9354	0.9583	0.9528	0.9717	0.9448	0.9874	0.9000	0.9829
Panel C: Model (6.10)								
$g_k(\cdot) \sim (6.7)$	0.8696	0.8139	0.8466	0.9608	0.7904	0.8105	0.6683	0.9892
$g_k(\cdot) \sim (6.12)$	0.9407	0.9440	0.9441	0.9792	0.9573	0.9782	0.9329	0.9923

Finally, we report the parameter estimation results for models (6.8), (6.9), and (6.10) in Table 6, when $g_h(\cdot)$, $g_s(\cdot)$, and $g_k(\cdot)$ satisfy the specifications in (6.3), (6.11), and (6.12), respectively. From Table 6, we can get the following important findings:

1. All of examined h_t , s_t , and k_t are persistent, since the estimated values of θ_h , θ_s , and θ_k are very large in all fitted models.
2. The estimated value of $\vartheta_{h,2}$ in each fitted $g_h(\cdot)$ is positive, implying that the negative past shocks have a larger impact on h_t than the positive past shocks. This is the well-known leverage effect on h_t in the literature. Since the estimated value of $\vartheta_{s,2}$ in each fitted $g_s(\cdot)$ is positive, s_t also has the leverage effect caused by the past re-scaled shocks. However, this leverage effect on s_t seems very weak (with the value of estimated $\vartheta_{s,2}$ equal to 0.0077) for the N225 return series. Indeed, the positive past re-scaled shocks have an optimistic impact on s_t for this return series, meaning that the investors in Japanese

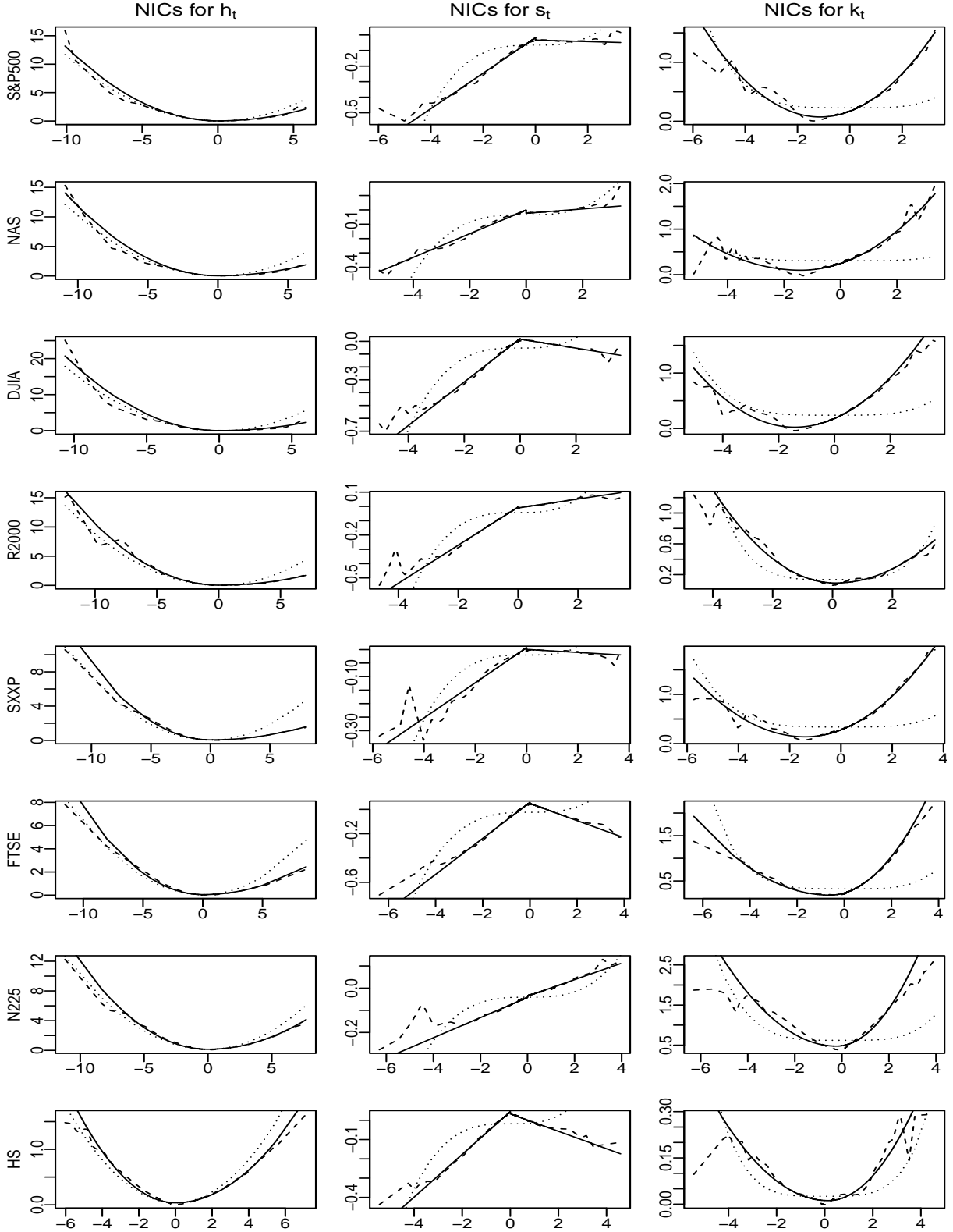


Fig 3: The plots of all fitted NICs for h_t , s_t , and k_t . Left panels: the non-parametric $\hat{g}_h(\cdot)$ (dashed lines); the parametric $g_h(\cdot)$ in (6.2) (dotted lines) and (6.3) (solid lines). Middle panels: the non-parametric $\hat{g}_s(\cdot)$ (dashed lines); the parametric $g_s(\cdot)$ in (6.6) (dotted lines) and (6.11) (solid lines). Right panels: the non-parametric $\hat{g}_k(\cdot)$ (dashed lines); the parametric $g_k(\cdot)$ in (6.7) (dotted lines) and (6.12) (solid lines).

market have an increasing chance to encounter extremely positive returns in the future when the market is rising now. A possible reason for this observation is that the N225 index has the low value of price/earnings ratio, so its investors may not worry too much about market bubble in a rising trend.

3. Compared with h_t and s_t , the leverage effect on k_t seems more vague in general (with the values of estimated $\vartheta_{k,2}$ around zero for S&P500, DJIA, SXXP, and HS return series). Besides this difference, k_t exhibits a unique “non-zero kink” phenomenon that the minimizer of its fitted $g_k(\cdot)$ is not zero, particularly for the S&P500, NAS, DJIA, SXXP, and FTSE return series (with the values of estimated $\vartheta_{k,3}$ larger than 0.5). This “non-zero kink” phenomenon seems new to the literature, implying that some small negative but non-zero past re-scaled shocks have the weakest influence on the tail risk of having extreme returns. This phenomenon may be relevant to the “buy the dip” strategy used by institutional investors (Bonini et al., 2022). Since the small cap markets are more often affected by the retail investors, it is expected that the “non-zero kink” phenomenon is less evident in the R2000, N225, and HS return series than the other five return series from large cap markets.

7. Concluding Remarks. This paper estimates the three CMs (with respect to variance, skewness, and kurtosis) by the corresponding QCMs, which are easily computed from the OLS estimator of a linear regression model constructed by the ECQs. The QCM method builds on the Cornish-Fisher expansion, which essentially transforms the estimation of CM to that of conditional quantile. Such transformation brings us two attractive advantages over the parametric GARCH-type methods: First, the QCM method bypasses the investigation of conditional mean and allows the mis-specified conditional quantile models, due to its regression-based feature; Second, the QCM method has stable estimation results, since it does not involve any complex nonlinear constraint on the admission region of parameters in conditional quantile models.

TABLE 6
The estimation results for models (6.8)–(6.10).

	S&P500	NAS	DJIA	R2000	SXXP	FTSE	N225	HS
Panel A: Model (6.8) with $g_h(\cdot) \sim (6.3)$								
θ_h	0.8894 (0.0017)	0.8924 (0.0015)	0.8790 (0.0021)	0.9141 (0.0017)	0.9021 (0.0017)	0.9133 (0.0014)	0.8381 (0.0017)	0.9345 (0.0009)
$\vartheta_{h,0}$	0.0177 (0.0034)	0.0390 (0.0034)	−0.0009 (0.0051)	0.0302 (0.0055)	0.0471 (0.0026)	0.0363 (0.0020)	0.1251 (0.0038)	0.0292 (0.0015)
$\vartheta_{h,1}$	0.0594 (0.0017)	0.0457 (0.0013)	0.0608 (0.0027)	0.0319 (0.0015)	0.0214 (0.0010)	0.0300 (0.0008)	0.0653 (0.0008)	0.0360 (0.0004)
$\vartheta_{h,2}$	0.0687 (0.0017)	0.0712 (0.0014)	0.1216 (0.0029)	0.0724 (0.0016)	0.0655 (0.0011)	0.0436 (0.0008)	0.0507 (0.0009)	0.0214 (0.0004)
Panel B: Model (6.9) with $g_s(\cdot) \sim (6.11)$								
θ_s	0.8599 (0.0045)	0.9185 (0.0036)	0.8527 (0.0038)	0.8662 (0.0030)	0.9364 (0.0041)	0.9063 (0.0019)	0.8549 (0.0056)	0.9211 (0.0023)
$\vartheta_{s,0}$	−0.0234 (0.0025)	−0.0114 (0.0019)	0.0198 (0.0020)	−0.0070 (0.0014)	0.0050 (0.0017)	0.0546 (0.0008)	−0.0389 (0.0019)	0.0400 (0.0008)
$\vartheta_{s,1}$	−0.0129 (0.0017)	0.0037 (0.0013)	−0.0370 (0.0018)	0.0283 (0.0013)	−0.0087 (0.0015)	−0.0748 (0.0009)	0.0398 (0.0012)	−0.0502 (0.0008)
$\vartheta_{s,2}$	0.1225 (0.0025)	0.0717 (0.0019)	0.2048 (0.0028)	0.1027 (0.0020)	0.0717 (0.0023)	0.2197 (0.0014)	0.0077 (0.0020)	0.1569 (0.0012)
Panel C: Model (6.10) with $g_k(\cdot) \sim (6.12)$								
θ_k	0.9433 (0.0043)	0.9299 (0.0042)	0.9384 (0.0041)	0.9570 (0.0025)	0.9165 (0.0036)	0.9205 (0.0025)	0.8182 (0.0046)	0.9932 (0.0015)
$\vartheta_{k,0}$	0.0662 (0.0177)	0.0794 (0.0176)	0.0221 (0.0172)	0.0832 (0.0088)	0.1302 (0.0146)	0.1795 (0.0106)	0.5422 (0.0179)	0.0100 (0.0062)
$\vartheta_{k,1}$	0.0745 (0.0012)	0.0743 (0.0008)	0.0763 (0.0010)	0.0506 (0.0017)	0.0719 (0.0006)	0.1259 (0.0008)	0.1880 (0.0017)	0.0234 (0.0007)
$\vartheta_{k,2}$	0.0011 (0.0031)	−0.0210 (0.0038)	0.0056 (0.0048)	0.0217 (0.0018)	−0.0090 (0.0026)	−0.0740 (0.0013)	−0.0948 (0.0021)	−0.0095 (0.0007)
$\vartheta_{k,3}$	1.1377	1.4092	1.4316	−0.0916	1.3932	0.6047	0.2316	−0.1439

† The standard deviations of all parameters are shown in parentheses. Here, the standard deviations of the threshold parameter $\vartheta_{k,3}$ are absent, since the estimator of $\vartheta_{k,3}$ is not asymptotically normal (see, e.g., Chan (1993)).

The price of these two advantages is that we need to do the conditional quantile estimation n different times. But this seems neither a computational burden nor a theoretical obstruct. More importantly, the QCM method is a supervised learning procedure without assuming any distribution on the returns. This supervised learning feature makes the QCM method have a substantially computational advantage over the GARCH-type methods to estimate conditional variance, skewness, and kurtosis, when the dimension of return is large. See [Zhu et al. \(2023\)](#) for an in-depth discussion on this context and an innovative method for big portfolio selections based on the learned conditional higher-moments from the QCM method.

Finally, we should mention that the existing parametric methods commonly only work for stationary data and their extension to deal with more complex data environments seems challenging in terms of methodology and computation. In contrast, the QCM method could be applicable in complex data environments, as long as the ECQs are fairly provided. For example, the QCMs could adapt to the mixed categorical and continuous data or locally stationary data when the ECQs are computed by the method in [Li and Racine \(2008\)](#) or [Zhou and Wu \(2009\)](#), respectively. In addition, the useful information from exogenous variables and conditional quantiles of other variables can be easily embedded to the QCMs through the channels of the ECQs as done in [Härdle et al. \(2016\)](#) and [Tobias and Brunnermeier \(2016\)](#). Since the QCMs are computed at each fixed timepoint, the QCM method also allows us to pay special attention to the CMs during a specific time period by employing the methods in [Cai \(2002\)](#) and [Xu \(2013\)](#) to compute the ECQs. On the whole, the QCM method exhibits a much wider application scope than the parametric ones, which so far have not offered a clear feasible manner to study the CMs under the above complex data environments.

References.

- Andrews, D. W. K. (1988). Laws of large numbers for dependent nonidentically distributed random variables. *Econometric Theory* **4**, 458–467.

- Bali, T. G., Mo, H. and Tang, Y. (2008). The role of autoregressive conditional skewness and kurtosis in the estimation of conditional VaR. *Journal of Banking & Finance* **32**, 269–282.
- Bollerslev, T. (1986). Generalized autoregressive conditional heteroskedasticity. *Journal of Econometrics* **31**, 307–327.
- Bonini, S., Shohfi, T. and Simaan, M. (2022). Buy the Dip? Working paper. Available at “<https://ssrn.com/abstract=3835376>”.
- Brooks, C., Burke, S. P., Heravi, S. and Persaud, G. (2005). Autoregressive conditional kurtosis. *Journal of Financial Econometrics* **3**, 399–421.
- Cai, Z. (2002). Regression quantiles for time series. *Econometric Theory* **18**, 169–192.
- Chan, K. S. (1993). Consistency and limiting distribution of the least squares estimator of a threshold autoregressive model. *Annals of Statistics* **21**, 520–533.
- Chunhachinda, P., Dandapani, K., Hamid, S. and Prakash, A. J. (1997). Portfolio selection and skewness: Evidence from international stock markets. *Journal of Banking & Finance* **21**, 143–167.
- Cornish, E. A. and Fisher, R. A. (1938). Moments and cumulants in the specification of distributions. *Revue de l'Institut international de Statistique* **5**, 307–320.
- Engle, R. F. (1982). Autoregressive conditional heteroscedasticity with estimates of the variance of United Kingdom inflation. *Econometrica* **50**, 987–1007.
- Engle, R. F. and Manganelli, S. (2004). CAViaR: Conditional autoregressive value at risk by regression quantiles. *Journal of Business & Economic Statistics* **22**, 367–381.
- Engle, R. F. and Ng, V. K. (1993). Measuring and testing the impact of news on volatility. *Journal of Finance* **48**, 1749–1778.
- Escanciano, J. C. (2006). Goodness-of-fit tests for linear and nonlinear time series models. *Journal of the American Statistical Association* **101**, 140–149.
- Escanciano, J. C. (2009). Quasi-maximum likelihood estimation of semi-strong GARCH models. *Econometric Theory* **25**, 561–570.
- Escanciano, J. C. and Velasco, C. (2006). Generalized spectral tests for the martingale difference hypothesis. *Journal of Econometrics* **134**, 151–185.
- Fan, J. and Yao, Q. (2003). *Nonlinear Time Series: Nonparametric and Parametric Methods*. Springer, New York.
- Francq, C. and Sucarrat, G. (2022). Volatility estimation when the zero-process is nonstationary. *Journal of Business & Economic Statistics* **41**, 53–66.

- Francq, C. and Thieu, L. Q. (2019). QML inference for volatility models with covariates. *Econometric Theory* **35**, 37–72.
- Francq, C. and Zakoïan, J. M. (2019). *GARCH Models: Structure, Statistical Inference and Financial Applications*. John Wiley & Sons.
- Glosten, L. R., Jagannathan, R. and Runkle, D. E. (1993). On the relation between the expected value and the volatility of the nominal excess return on stocks. *Journal of Finance* **48**, 1779–1801.
- Grigoletto, M. and Lisi, F. (2009). Looking for skewness in financial time series. *Econometrics Journal* **12**, 310–323.
- Gu, S., Kelly, B. and Xiu, D. (2020). Empirical asset pricing via machine learning. *Review of Financial Studies* **33**, 2223–2273.
- Haas, M., Mittnik, S. and Paolella, M. S. (2004). Mixed normal conditional heteroskedasticity. *Journal of Financial Econometrics* **2**, 211–250.
- Hansen, B. E. (1994). Autoregressive conditional density estimation. *International Economic Review* **35**, 705–730.
- Härdle, W. K., Wang, W. and Yu, L. (2016). TENET: Tail-Event driven NETwork risk. *Journal of Econometrics* **192**, 499–513.
- Harvey, C. R. and Siddique, A. (1999). Autoregressive conditional skewness. *Journal of Financial and Quantitative Analysis* **34**, 465–487.
- Harvey, C. R. and Siddique, A. (2000). Conditional skewness in asset pricing tests. *Journal of Finance* **55**, 1263–1295.
- Jondeau, E. and Rockinger, M. (2003). Conditional volatility, skewness, and kurtosis: existence, persistence, and comovements. *Journal of Economic Dynamics and Control* **27**, 1699–1737.
- Jondeau, E., Zhang, Q. and Zhu, X. (2019). Average skewness matters. *Journal of Financial Economics* **134**, 29–47.
- Koenker, R. and Bassett, G. (1978). Regression quantiles. *Econometrica* **46**, 33–50.
- Koenker, R., Chernozhukov, V., He, X. and Peng, L. (2017). *Handbook of Quantile Regression*. Chapman & Hall/CRC.
- Kuester, K., Mittnik, S. and Paolella, M. S. (2006). Value-at-risk prediction: A comparison of alternative strategies. *Journal of Financial Econometrics* **4**, 53–89.
- León, Á. and Níguez, T. M. (2020). Modeling asset returns under time-varying semi-nonparametric distributions. *Journal of Banking & Finance* **118**, 105870.

- León, Á., Rubio, G. and Serna, G. (2005). Autoregressive conditional volatility, skewness and kurtosis. *Quarterly Review of Economics and Finance* **45**, 599–618.
- Li, Q. and Racine, J. S. (2008). Nonparametric estimation of conditional CDF and quantile functions with mixed categorical and continuous data. *Journal of Business & Economic Statistics* **26**, 423–434.
- Ljung, G. M. and Box, G. E. (1978). On a measure of lack of fit in time series models. *Biometrika* **65**, 297–303.
- McNeil, A. J. and Frey, R. (2000). Estimation of tail-related risk measures for heteroscedastic financial time series: an extreme value approach. *Journal of Empirical Finance* **7**, 271–300.
- Robinson, P. M. (1988). Root-N-consistent semiparametric regression. *Econometrica* **56**, 931–954.
- Rubinstein, M. E. (1973). A comparative statics analysis of risk premiums. *Journal of Business* **46**, 605–615.
- Samuelson, P. A. (1970). The fundamental approximation theorem of portfolio analysis in terms of means, variances and higher moments. *Review of Economic Studies* **37**, 537–542.
- Sgouropoulos, N., Yao, Q. and Yastremiz, C. (2015). Matching a distribution by matching quantiles estimation. *Journal of the American Statistical Association* **110**, 742–759.
- Sucarrat, G. and Grønneberg, S. (2022). Risk estimation with a time-varying probability of zero returns. *Journal of Financial Econometrics* **20**, 278–309.
- Tobias, A. and Brunnermeier, M. K. (2016). CoVaR. *American Economic Review* **106**, 1705–1741.
- Tong, H. (1978). On a threshold model. *Pattern recognition and signal processing*. (ed. C.H.Chen). Sijthoff and Noordhoff, Amsterdam.
- Tsay, R. S. (2005). *Analysis of Financial Time Series*. John Wiley & Sons.
- White, H. (2001). *Asymptotic Theory for Econometricians, Revised edition*. San Diego: Academic Press.
- Widder, D. V. (1946). *The Laplace Transform*. Princeton University Press, Princeton, NJ.
- Xiao, Z. and Koenker, R. (2009). Conditional quantile estimation for generalized autoregressive conditional heteroscedasticity models. *Journal of the American Statistical Association* **104**, 1696–1712.
- Xu, K. L. (2013). Nonparametric inference for conditional quantiles of time series. *Econometric Theory* **29**, 673–698.
- Zheng, Y., Zhu, Q., Li, G. and Xiao, Z. (2018). Hybrid quantile regression estimation for time series models with conditional heteroscedasticity. *Journal of the Royal Statistical Society: Series B* **80**, 975–993.
- Zhou, Z. and Wu, W. B. (2009). Local linear quantile estimation for nonstationary time series. *Annals of Statistics* **37**, 2696–2729.
- Zhu, Z., Zhang, N. and Zhu, K. (2023). Big portfolio selection by graph-based conditional moments method. Working paper. Available at “<https://arxiv.org/abs/2301.11697>”.